Directed percolation effects emerging from superadditivity of quantum networks

L. Czekaj,[1,2] R. W. Chhajlany,[3,1,2] and P. Horodecki[1,2]

[1]*Faculty of Applied Physics and Mathematics, Gdańsk University of Technology, 80-952 Gdańsk, Poland*

[2]*National Quantum Information Center of Gdańsk, 81-824 Sopot, Poland*

[3]*Faculty of Physics, Adam Mickiewicz University, Umultowska 85, 61-614 Poznań, Poland*

(Received 6 July 2011; revised manuscript received 16 January 2012; published 26 March 2012)

Entanglement-induced nonadditivity of classical communication capacity in networks consisting of quantum channels is considered. Communication lattices consisting of butterfly-type entanglement-breaking channels augmented, with some probability, by identity channels are analyzed. The capacity superadditivity in the network is manifested in directed correlated bond percolation which we consider in two flavors: simply directed and randomly oriented. The obtained percolation properties show that high-capacity information transfer sets in much faster in the regime of superadditive communication capacity than otherwise possible. As a by-product, this sheds light on a type of entanglement-based quantum capacity percolation phenomenon.

DOI: 10.1103/PhysRevA.85.032328 PACS number(s): 03.67.Hk, 64.60.ah, 89.70.Kn, 89.75.Hc

Introduction. Percolation (see, e.g., [1,2]) is a natural concept that emerges in the description of spreading processes in the presence of medium imperfections. Percolation effects in quantum networks have recently been the subject of increasing interest [3–7]. The focus has been on generation of large-scale networks with maximally entangled states between elementary nodes to allow for quantum communication applications, starting from initially imperfect, i.e., non–maximally entangled state, networks. The interesting central new insight introduced in [3,4] is that local quantum operations may be used not only to purify entanglement but, simultaneously, to lower percolation probability threshold by effectively changing lattice topology. This idea has been developed for different states [5,6] and lattice dimensions [7,8]. In a different context, percolation concepts also appeared in quantum information theory (QIT) in the study of cluster state generation [9].

The capacity of a network determines its utility in the domain of communication. The development of QIT has led to the uncovering of interesting quantum effects on channel capacities, e.g., superadditivity of quantum (Q-type) channel capacity [10]. This result followed the intuition developed in the bound entanglement activation effect [11] (where two weak resources activate each other becoming collectively useful for some task) continued further in Refs. [12] and [13]. Independently, the first superadditivity effect of classical (C-type) capacity in quantum multiaccess channels (MACs) has been described [14]. Remarkably, both Q-type and C-type superadditivities have recently been proved possible even for entanglement-breaking (EB) channels [15] in the MAC context. In contrast, EB bipartite channels do not exhibit superadditive phenomena [16], showing that multipartite channels represent fundamentally different resources for communication than bipartite ones.

In this paper, we consider percolation effects in quantum networks from (i) a channel (not the common state [3]) perspective, (ii) using MACs as communication resources. We present schemes of classical information transfer (C-type) through quantum MAC networks, which can be mapped to certain types of *directed* bond percolation problems [17]. We first consider a simple layered communication scheme (A) to demonstrate the basic idea of percolation assisted by superadditive capacities and then describe a more complicated scheme of multidirectional communication (B). Interestingly, the percolation problem in case B seems relatively unstudied in the literature.

a. The basic tools. We shall consider a network consisting of two superimposed networks, a passive one and an active one (see Fig. 1). The passive network is the fixed, underlying network and is built up of elementary entanglement-breaking MACs, where no bond allows *a priori* high-capacity communication (HCC). The active network is an auxiliary, incomplete network consisting of randomly generated (open) bonds representing high-capacity channels. Importantly, we choose the active channels so that they can serve to activate HCC through the passive channels, as summarized below.

The elementary channel of the passive network is chosen in this paper as a 2-sender $(N_{i,t}, N_{i+1,t})$ 1-receiver $(N_{i,t+1})$ noisy quantum MAC depicted as the wedge-shaped channel in Fig. 1(b): The slanted line is a two-qudit (d^2-dimensional) input pertaining to one user $N_{i+1,t}$; the vertical line is a single-qudit input of the second user $N_{i,t}$. The action of the channel is such that the single-qudit system undergoes a controlled operation from a chosen set of orthogonal d^2 unitary operations fired by the logical value of the two-qudit input state of $N_{i+1,t}$ (see Ref. [15] for details). This single-qudit line is further modified by a depolarizing channel and is the sole output system at the $N_{i,t+1}$ receiver output. For moderate to large depolarization—the working regime considered here—this channel has poor classical capacity C' for any user [15]:

$$C' \ll C_0 \leqslant C_{\max} \equiv \log_2 d, \tag{1}$$

where $C_{\max}$ is the maximal attainable capacity for a single-qudit output, corresponding to an identity channel. Note finally that the passive channel allows for one-way communication only, and so induces a sense of direction of communication.

Communication properties can be improved by adding a high-capacity active channel, e.g., an ideal channel, along the vertical transmission line, i.e., between $N_{i,t}$ and $N_{i,t+1}$. On the one hand, this trivially increases the capacity of $N_{i,t} \to N_{i,t+1}$. Alternatively, and more importantly, even though $N_{i+1,t}$ does not directly have access to the active channel, user $N_{i,t}$ can assist $N_{i+1,t}$ by inputting a two-party maximally entangled state to his inputs [entanglement-assisted scheme (EA)], i.e., the ideal channel and vertical line of the wedge channel in

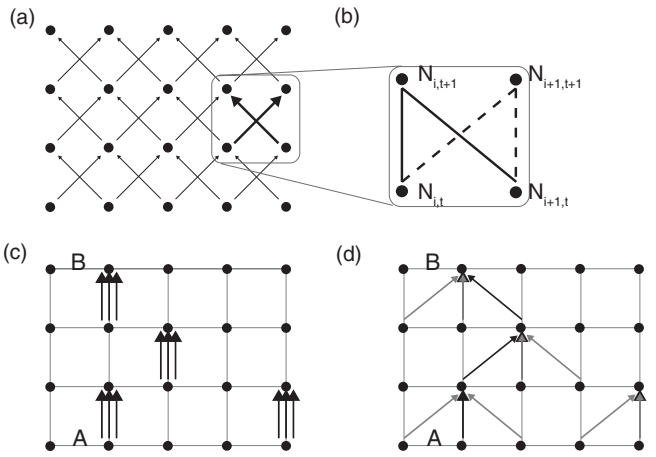

FIG. 1. Model A: layered communication network. (a) Passive network; users are located at nodes of a square lattice, the lattice is filled with butterfly shaped primitives, information flow is directed from layer $t \to t+1$. (b) Butterfly primitive consists of two MACs (solid and dashed wedges) from Ref. [15]; node (user) $N_{i,t}$ can communicate with $N_{i-1,t+1}, N_{i,t+1}, N_{i+1,t+1}$ with maximal capacity $C' \ll C_0$. (c) Active network filled randomly by triples of ideal channels allowing HCC (shown is a configuration not allowing HCC from A to B). (d) Entanglement activates the slanted lines of the corresponding passive channels (a) for HCC using dense coding, and thus changes the geometry of the initial HCC network (c) leading to directed communication paths (black arrows) with capacities $\geqslant C_0$ from A to B.

Fig. 1(b). By construction of the passive channel described above, this enables user $N_{i+1,t}$ to perform dense coding of inputs transmitted to $N_{i,t+1}$ and thus increase the capacity on the $N_{i+1,t} \to N_{i,t+1}$ line to some much higher value $C_0 > C'$ [22]. This is a manifestation of superadditivity of channel capacities (for high depolarization when the channel becomes entanglement breaking, $C_0 \approx (d+1)C'$ [15]). We define HCC as transmission at a rate $\geqslant C_0$.

b. Model A: Layered network communication. In the network context, we first consider the scenario where only forward communication is allowed (see Fig. 1). The passive channel inputs are shared by nearest-neighbor pairs of sites in horizontal layers giving rise to a butterfly-shaped fixed network. The active channels are only placed on vertical bonds. We shall suppose that these are available with probability p—one can assume that identity channels are initially available at all vertical bonds, yet due to fragility with respect to noise either remain useful (ideal) with probability p (open bonds) or become unuseful random operations with probability $1-p$ (closed bonds) effectively erasing information. In our scheme, we consider a setup where a triple of identity channels is the basic active channel [23]—if present, this allows the possibility of simultaneous HCC between a given sender and his vertically placed receiver, through one identity channel, as well as between the sender's two horizontal nearest neighbors and that receiver [Figs. 1(c) and 1(d)] activated by the remaining two identity channels.

The question of establishing long-range HCC in such a network is a directed percolation problem. One asks, under what conditions is it possible for any user to be able to perform directed HCC, through intermediate nodes, with a user or users located at a distance scaling with the length of the network? One may compare two scenarios: (a) entanglement free or classical, where no entanglement is allowed in the protocol used at any node, and (b) entanglement assisted (EA), which takes full advantage of the superadditive effect based on dense coding as described earlier.

The former case corresponds to HCC only along the 1-dimensional paths of just the active lattice [see [22]; Fig. 1(c)] and the percolation threshold probability is 1, rendering the network useless for HCC for finite loss probability of active channels. The EA scheme involves changing the geometry of the HCC network due to activation of the slanted lines of the passive channels [Figs. 1(b) and 1(d)], from the active network of 1-dimensional chains to the 2-dimensional network of Fig. 1(d). This scheme thus maps to a *correlated* directed bond percolation problem where with probability p three directed bonds (forming an arrow shape) are placed on the lattice [Fig. 1(d)]. The threshold probability is significantly suppressed due to entanglement-activated increased connectivity. We performed a standard Monte Carlo simulation (see Appendix) and found the percolation threshold to be $p_c = 0.5388$ with accuracy $\Delta = 0.0005$. We have checked that the studied percolation transition lies, as expected, in the directed percolation (DP) universality class, by computing a complete set of critical exponents and found them to be in agreement with those obtained for the uncorrelated directed bond percolation problem. The important basic characteristic of directed percolation is that the connected clusters of nodes are geometrically highly asymmetrical and are restricted to acute cones (with cone angle $\pi/2$ when $p = 1$) with axes along the vertical lines passing through the starting nodes. Near the critical point the clusters are very narrow and essentially quasi-1-dimensional, as the probability of obtaining a connection with a site a large distance away from the source and at an angle θ from the axis $\Theta(p,\theta) > 0$ for $|\theta| < \delta\theta(p) \sim (p-p_c)^b$ (see, e.g., Dhar and Barma [18]). The EA scheme beats the classical scheme in that there is a wide window in p for HCC, and that the horizontal extent of connections $|\theta|$ at a distance $t \to \infty$ away changes from 0 to $\pi/4$ as p increases from p_c to 1.

c. Model B: Randomly oriented communication. We now move to a general scenario within the described framework of basic channels (Fig. 2). The basic active channels can be placed with probability p on any bond, connecting nearest neighbors, of the square lattice and are tagged for use in a particular direction. The passive channels are distributed on the lattice as shown in Fig. 2(b). Again, each (slanted line of a) passive channel can be activated by an active channel tagged for use in the same direction, by entanglement exactly as in model A giving rise to a complicated multidirectional random HCC network [Fig. 2(d)].

HCC between distant nodes is now a multidirectional bond percolation problem. We consider the case where upward and left-to-right oriented active channels are present with probability p_+ while downward and right-to-left oriented active channels are placed with probability p_-. Note that bidirectional bonds appear as the independent choice of two oppositely directed channels on a given bond.

This setup is interesting already for the case when, say, $p_- = 0$. Using an entanglement-free protocol (see comment [22]), capacity $C \geqslant C_0$ can already be attained only through

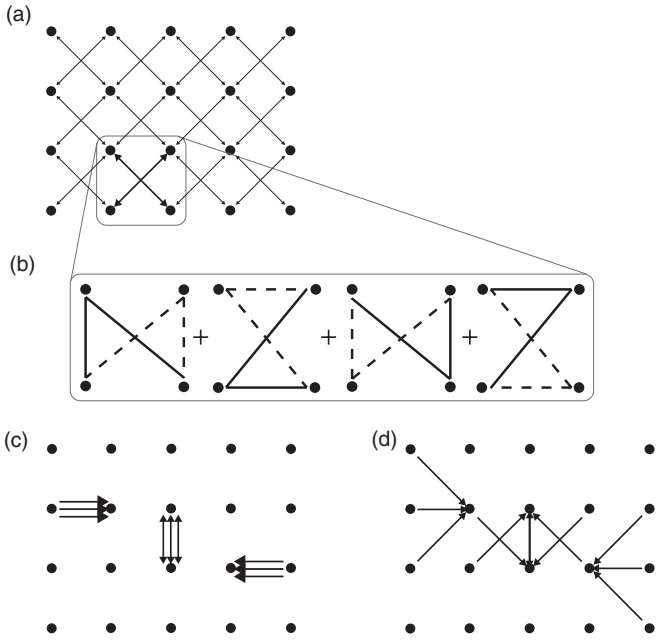

FIG. 2. Model B: multidirectional communication networks. (a) Passive network, allowing communication in each direction; (b) this is due to the structure of the butterfly primitive depicted here—each quartet of nodes forming an elementary square is connected by 4 passive channels, of the type shown in Fig. 1(b). (c) Active channels can be placed on any bond and tagged for use in any direction. (d) Emergent network geometry from superimposing (a) and (c), due to dense coding allowing HCC along slanted lines, facilitated by entanglement between active and passive channels.

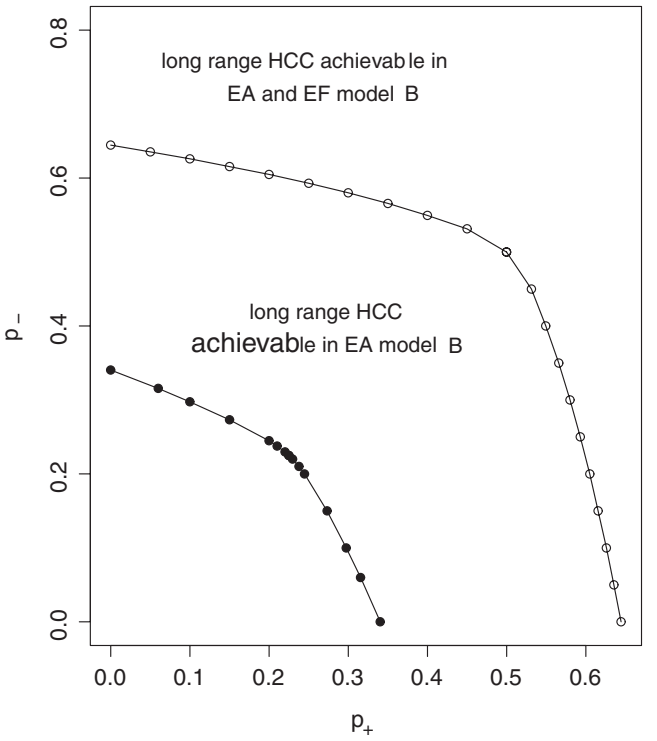

FIG. 3. Comparison of the percolation critical lines $[p_+^c, p_-^c(p_+^c)]$ for percolation process on randomly oriented square lattice (classical scheme) and butterfly network (EA scheme). Dots are numerically obtained points.

the square lattice using the active network in the up or right directions (without activating the passive network), in contrast to model A. This is the well-known square lattice directed bond percolation problem for which the percolation threshold $p_c \approx 0.64$ (see, e.g., [18]). Using on the other hand the EA scheme to activate the passive network, due to increased and correlated connectivity [Fig. 2(d)], the percolation threshold is almost halved with respect to the classical scheme and has been calculated here to be $p_c \approx 0.34$ using our Monte Carlo simulation (see Appendix). Both phase transitions lie in the DP universality class. Thus, e.g., at moderate noise levels $p \approx 0.6$, the probability of a starting node belonging to an infinite or system-spanning anisotropic cluster (in the thermodynamic limit) $F_\infty > 1/2$ using superadditivity effects while $F_\infty = 0$ otherwise.

The general multidirectional communication problem with arbitrary $p_\pm$ is the most interesting setup. In the classical, entanglement-free scenario, this reduces to square lattice randomly oriented percolation in the active network [22]. Problems of this category were studied in the context of random resistor diode networks (see, e.g., [19,20]) mainly using renormalization group calculations. However not many results seem to be available in the literature on the $p_\pm$ percolation problem (see however [21] for some analytical properties).

Here, we map out the phase diagram in the (p_+, p_-) plane in Fig. 3 using Monte Carlo simulations (see Appendix). Note that the diagram is symmetrical with respect to the line $p_+ = p_-$ due to system symmetry under the interchange $p_+ \leftrightarrow p_-$. The upper line is for the active network percolation problem (classical scheme). This result is to be compared with the multidirectional correlated bond percolation phase diagram for the EA scheme [network of Fig. 2(d)]. As can be seen in Fig. 3, the EA scheme is drastically better than the classical scheme in the whole parameter plane.

An interesting feature of both the classical and EA schemes is that they allow switching of universality classes of phase transitions from the DP class to the isotropic percolation (IP) class to which standard bond and site percolation belongs. This is facilitated by the choice of parameters $p_\pm$, and as a result one may accordingly change the properties of the long-range clusters. To provide evidence for this, we calculate two universal critical exponents (Fig. 4) β and the Fisher exponent τ (see Appendix) as one moves along the critical lines (Fig. 3) of the two models. Recall that β determines how the percolation probability $F_\infty \sim (p - p_c)^\beta$ increases above the percolation threshold, while the Fisher exponent determines how the probability of obtaining a cluster larger than size n decreases with n at the critical point $p = p_c$: $F_n \sim 1/n^{\tau-2}$. Note that the values of these exponents in the DP class are $\beta \approx 0.276, \tau \approx 2.112$ [18], and in IP $\beta = 5/36 \approx 0.139, \tau = 187/91 \approx 2.0549$ [1]. First consider square lattice multidirectional percolation in Fig. 4 (the classical scheme). Both exponents show that as one moves along the critical line, the phase transitions lie in the DP universality class until $p_-^c \approx 0.4$, since this region inherits the exponents of the DP point $p_-^c = 0$. At $p_-^c = 1/2$ $(= p_+^c)$, which is an isotropic symmetry point, one obtains values of the exponents

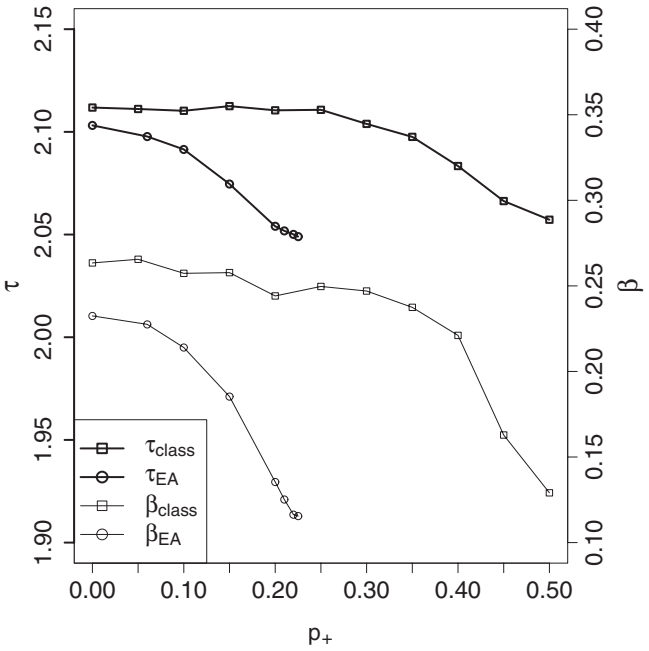

FIG. 4. Comparison of critical exponents τ, β for classical and EA schemes of multidirectionally oriented percolation.

corresponding to the IP universality class. In between, there is a characteristic crossover region between the two types of behavior. In particular, this means that for a choice of parameters approaching the isotropic point, one obtains different characteristic growth of clusters (determined by different critical exponents) than when in the DP region. Second, the cluster geometrical characteristics change from highly anisotropic to isotropic. The butterfly network percolation problem (EA scheme) basically follows the same pattern (see Fig. 4) and can be considered a rescaled version of the classical problem, wherein again lies the quantum advantage of the EA scheme. For this network, the isotropy point is found to be located at $p_+^c = p_-^c \approx 0.225$. The slightly lower values of β in the DP regime as compared to the square lattice problem do not seem to be significant, and are a result of the extreme sensitivity of the calculated exponents on the accuracy of critical probabilities.

Concluding remarks. We have described percolation effects in a channel context showing how directed percolation effects emerge in the consideration of quantum networks. In the context of percolation theory, the multidirectional correlated bond percolation problem associated with the entanglement - assisted (EA) scheme has, to our knowledge, not been studied before.

Finally, quite remarkably, our results provide an entanglement percolation effect in the spirit of Ref. [3]. Keeping everything else unchanged, consider the Bell measurement (BM) MAC of Fig. 1 of Ref. [15] instead of the MAC used here, with AC (BC) playing the role of diagonal (resp. vertical) bond of the square lattice. Then any randomly generated singlet between B and C can be switched, via entanglement swapping, to a singlet on the diagonal AC. This leads to the same geometry as discussed here but now one asks about the possibility of building a long-range network of singlets. Note that singlets are directionless. Without using the BM channel, we obtain a "classical" scheme related to square lattice percolation which has threshold $p_c = 0.5$. Since directionless percolation must certainly be at least as good as directed percolation, an EA scheme making use of the switching mechanism of the BM channel will have threshold at most equal to the calculated threshold at the isotropic point of model B $p_c^{EA} \leqslant p_+^c = p_-^c \approx 0.225$.

Acknowledgments.The authors thank J. K. Korbicz for discussions. P.H. thanks also C. H. Bennett and A. Grudka for discussions. The work was supported by EU project QESSENCE and by the Polish Ministry of Science and Higher Education through Grant No. NN202231937. Part of the work was done at the Quantum Information Centre of Gdansk.

APPENDIX

The critical percolation properties of the two models were studied using direct Monte Carlo simulations in the spirit of Dhar and Barma [18]. We studied the change in behavior of the probability F_n, of appearance of clusters of size greater than n, with bond probabilities p and looked for characteristic scaling behavior expected in the critical region to identify percolation thresholds plotted. Below the probability threshold, $F_n \propto \exp(-n)$ for large n while $F_n \to$ constant in the supercritical phase [1]. The critical region is characterized by scaling laws with $F_n \propto n^{2-\tau}$ described by a power-law dependence at the critical value p_c, which we localized by sweeping through super- and subcritical probabilities using an interval bisection method. For model A, cluster size distribution data were obtained by performing 10^5 realizations (per value of probability p) of cluster growth starting from a single node. Model B simulations were performed on a fixed 2×10^3 by 2×10^3 square lattice also with 10^5 realizations for each p, where cluster connectivity was identified using a breadth-first search algorithm.

The qualitative values of the critical exponents τ, β presented in the paper for model B are defined as follows:

$$F_n(p) \sim n^{-(\tau-2)} \text{ at } p = p_c$$

and

$$F_\infty(p) \sim (p - p_c)^\beta.$$

A simple method used to obtain these was to directly calculate the slope of the plots of these two functions in log-log scale. Since the problem contains two parameters p_+, p_-, we chose one of them p_+ do be the independent parameter with $p_-(p_+)$ determined so as to be on the critical line of the model. For the determination of β, we considered clusters of size n greater than 10^5 to be "infinite" or system-spanning clusters on the finite lattice.

Alternatively, we also determined β from τ and an auxiliary exponent γ, which describes the critical behavior of mean cluster size $\langle n \rangle$ also readily available from the simulation:

$$\langle n \rangle \sim (p_c - p)^{-\gamma} \text{ for } p - p_c \to 0^+.$$

The following universal equation, derived from scaling relations, is known to hold for directed (uncorrelated) bond

percolation [18] and isotropic percolation [1]:

$$\beta = \left(\frac{\tau - 2}{3 - \tau}\right)\gamma.$$

We assumed the equation to be true for the entire critical plane and obtained results for β in agreement with those obtained using the first method. Results obtained in the latter manner are those presented in the paper.

[1] D. Stauffer and A. Aharony, *Introduction to Percolation Theory* (Taylor & Francis, London, 2003).

[2] G. Grimmett, *Percolation* (Springer-Verlag, Berlin, 1999).

[3] A. Acin, J. I. Cirac, and M. Lewenstein, Nature Phys. **3**, 256 (2007).

[4] G. J. Lapeyre Jr., J. Wehr, and M. Lewenstein, Phys. Rev. A **79**, 042324 (2009).

[5] S. Perseguers, L. Jiang, N. Schuch, F. Verstraete, M. D. Lukin, J. I. Cirac, and K. G. H. Vollbrecht, Phys. Rev. A **78**, 062324 (2008); S. Perseguers, D. Cavalcanti, G. J. Lapeyre Jr., M. Lewenstein, and A. Acin, *ibid*. **81**, 032327 (2010).

[6] S. Broadfoot, U. Dorner, and D. Jaksch, Europhys. Lett. **88**, 50002 (2009).

[7] S. Perseguers, Phys. Rev. A **81**, 012310 (2010).

[8] A. Grudka *et al*. (unpublished).

[9] K. Kieling and J. Eisert, in *Quantum and Semiclassical Percolation and Breakdown in Disordered Solids* (Springer, Berlin, 2009), pp. 287–319.

[10] G. Smith and J. Yard, Science **321**, 1812 (2008).

[11] P. Horodecki, M. Horodecki, and R. Horodecki, Phys. Rev. Lett. **82**, 1056 (1999).

[12] P. W. Shor, J. A. Smolin, and A. V. Thapliyal, Phys. Rev. Lett. **90**, 107901 (2003).

[13] W. Dür, J. I. Cirac, and P. Horodecki, Phys. Rev. Lett. **93**, 020503 (2004).

[14] L. Czekaj and P. Horodecki, Phys. Rev. Lett. **102**, 110505 (2009).

[15] A. Grudka and P. Horodecki, Phys. Rev. A **81**, 060305(R) (2010).

[16] M. Horodecki, P. W. Shor, and M. B. Ruskai, Rev. Math. Phys. **15**, 629 (2003).

[17] S. R. Broadbent and J. M. Hammersley, Proc. Cambridge Philos. Soc. **53**, 629 (1957).

[18] D. Dhar and M. Barma, J. Phys. C **14**, L1 (1981).

[19] H. Hinrichsen, Adv. Phys. **49**, 815 (2000).

[20] S. Redner, J. Phys. A: Math. Gen. **14**, L349 (1981); **15**, L685 (1982); Phys. Rev. B **25**, 3242 (1982).

[21] Geoffrey R. Grimmett, Random Structures & Algorithms **18**, 257 (2001).

[22] Note that product state encodings by user $N_{i,t}$ do not allow any information flow (zero capacity) from user $N_{i+1,t}$ through the identity channel since it is inaccessible to the latter. Thus, in this case the total capacity attainable by $N_{i,t+1}$ through the combination of the active and passive channel is still C'.

[23] For qubit channels, e.g., this can be physically realized as a process of ideal transmission with probability p of a single photon having three frequency states and two polarization degrees of freedom for each frequency, where the dominating noise process is photon loss.